Available online at www.sciencedirect.com
SCIENCE DIRECT®
Vision Research 44 (2004) 2019–2026
Vision Research
www.elsevier.com/locate/visres

Distribution of short-wavelength-sensitive cones in human fetal and postnatal retina: early development of spatial order and density profiles

Elisa E. Cornish [a,*], Anita E. Hendrickson [b], Jan M. Provis [a,c]

[a] Department of Clinical Ophthalmology C09, Save Sight Institute, University of Sydney, Sydney, NSW 2006, Australia
[b] Department of Biological Structure, University of Washington, Seattle, WA 98195, USA
[c] Department of Anatomy and Histology, University of Sydney, NSW 2006, Australia

Received 29 September 2003; received in revised form 20 February 2004

Abstract

We analysed spatial density and distribution of short-wavelength-sensitive photoreceptors (S-cones) in developing and adult human retinae using antibody against short-wavelength-sensitive opsin. Statistical tests indicate that before 20 weeks of gestation (WG) the S-cone mosaic is not distinguishable from a random distribution, but by 20 WG is significantly different from a random distribution in the perifoveal region, as reported previously for adult retina. Changes in spatial density during development are consistent with displacement of the photoreceptor population towards the incipient fovea so that prior to 20 WG, peak S-cone density is >1.7 mm from the fovea, but is within 800 μm of the fovea by 20 WG.

Keywords: Cones; Spatial distribution; Spatial order; Development; Displacement

1. Introduction

In primates, the majority of cones at the fovea provide input to midget pathways that mediate high acuity and color vision. At the adult fovea cones are packed at very high density, established as a result of displacement of photoreceptors towards the developing fovea during pre- and postnatal development (Diaz-Araya & Provis, 1992; Hendrickson & Kupfer, 1976; Yuodelis & Hendrickson, 1986). This displacement has been inferred from measurement of the diameter of the 'rod free' region, which *decreases* in size as development progresses (Hendrickson & Kupfer, 1976; Yuodelis & Hendrickson, 1986), and from measurement of the spatial density of cones within the cone mosaic at the fovea, which *increases* during development (Diaz-Araya & Provis, 1992; Yuodelis & Hendrickson, 1986), in the absence of local cell division (Provis, van Driel, Billson, & Russell, 1985; Sandercoe, Madigan, Billson, Penfold, & Provis, 1999).

Throughout most of the adult human retina S-cones make up 8–10% of the cone population (Curcio et al., 1991; Marc & Sperling, 1977). However, S-cones are absent from the central 100 μm or so of the central fovea (Bumsted & Hendrickson, 1999; Curcio et al., 1991; Williams, MacLeod, & Hayhoe, 1981), and reach peak spatial density at 0.1–0.5 mm eccentricity, where they comprise 1.5–5.5% of the local cone population (Curcio et al., 1991). While it is generally agreed that centripetal displacement of photoreceptors is the mechanism leading to increases in cone density centrally, photoreceptor displacement has not previously been investigated directly in a sample population of photoreceptors. We recently established that after 17 weeks' gestation (WG) S-cones comprise 8–10% of cone photoreceptors in sample areas located near the optic disc (OD) (Cornish, Xiao, Yang, Provis, & Hendrickson, in press), suggesting that at this eccentricity S-cones form a stable sample cone population from an early age. Assuming that S-cones and long- and medium-wavelength-sensitive cones (L/M cones) do not significantly alter spatial

* Corresponding author. Tel.: +61-2-9382-7283; fax: +61-2-9382-7318.
E-mail address: leese@anatomy.usyd.edu.au (E.E. Cornish).

0042-6989/$ - see front matter © 2004 Elsevier Ltd. All rights reserved.
doi:10.1016/j.visres.2004.03.030

relationships with one another during development, changes in the density distribution of S-cones during photoreceptor displacement will reflect changes in the distribution of the cone population as a whole.

Several studies have addressed the question of order in the arrangement of S-cones in adult human retina, using different approaches. Those studies indicate that within 0.5 mm of the central fovea the spatial order of S-cones cannot be distinguished from a random distribution, but that at locations more distant from the fovea S-cones are more regularly distributed (Ahnelt, Kolb, & Pflug, 1987; Curcio et al., 1991; Martin, Grunert, Chan, & Bumsted, 2000; Roorda, Metha, Lennie, & Williams, 2001; Roorda & Williams, 1999;). The spatial order of S-cones in developing retina, however, has not been investigated previously.

In this study we investigate changes in both spatial density and order in the distribution of S-cones in human fetal retinae. Because retinae under the age of 25 WG do not have a foveal depression, but show clearly the virtually rod and S-cone free cone mosaic at the fovea from an early age, we use 'foveal cone mosaic' (FCM) to identify the foveal region in both prefoveate and foveate specimens. Since several studies have shown that the region of retina surrounding the OD and extending out to the FCM changes relatively little during development (Packer, Hendrickson, & Curcio, 1990; Provis & van Driel, 1985; Robinson & Hendrickson, 1995; Steineke & Kirby, 1993) we have used a sample region stretching between and including the OD and FCM in all retinae analysed. Within that region, sample areas between 0.2 and 0.5 mm eccentricity are defined as being from the foveal 'rim', and sample regions from 1.5–3.0 mm eccentricity as being from the 'perifovea'. We did not sample areas from the 'parafovea' (1.0–1.5 mm eccentricity). Analyses of S-cone distributions in this strip over time show (1) a marked change in S-cone spatial density distribution between 17 WG and adulthood, and (2) that initially S-cones are randomly distributed throughout the sample strip, but are significantly different from a random array in the perifovea by 20 WG.

2. Materials and methods

2.1. Tissue

Six fetal eyes (17, 18, 18, 19, 20, 24 WG), one juvenile (6 weeks postnatal) and one adult (82 years) were used in this study. Studies were carried out using protocols approved by both the Human Subjects Committees of University of Washington and the Human Ethics Committee of the University of Sydney. Fetal eyes of known gestational age were obtained from surgical terminations carried out in the Sydney metropolitan area, or through the Human Embryology Laboratory, University of Washington or ABR, Inc., Alameda, CA. Gestational age was confirmed by *post mortem* estimates of retinal areas from previous studies (Provis et al., 1985). One juvenile eye was obtained with approval of the University of Washington through the Lions Eye Bank of the Northwest, WA, USA. The adult eye was obtained with ethical approval and informed consent via the Lions N.S.W. Eye Bank. Fetal tissue was immersion fixed in 2% paraformaldehyde in 0.1 M phosphate buffer (pH 7.4) for 30 min to 2 h. Juvenile and adult eyes were immersion fixed in 2% paraformaldehyde in 0.1 M phosphate buffered saline (PBS, pH 7.4) overnight. Anterior segments and vitreous were removed and the eye cups returned to fix. Retinae were then dissected free from the sclera, choroid and retinal pigment epithelium and postfixed for a further 24 h at 4 °C before further processing.

2.2. Immunohistochemistry

Whole retinae were rinsed in Tris-buffered saline (TBS, pH 7.6 containing sodium azide) overnight at 4 °C on a shaker table. Retinae were blocked in a solution containing 0.2% saponin *or* 0.2% triton and 10% normal goat serum (NGS) in TBS at 4 °C for 24–36 h. Polyclonal antibody to S-opsin was kindly donated by Nathans (Chiu, Zack, Wang, & Nathans, 1994; Wang et al., 1992). Whole retinae were incubated in anti-S-opsin (1:10,000 in TBS containing 0.2% saponin or 0.1% triton and 2% NGS) for 3–5 days at 4 °C. Bound antibody was detected using goat anti-rabbit IgG conjugated with Alexa 488 (1:1000 for 1–2 h; Molecular Probes). Retinae were washed in TBS and coverslipped in DABCO (6 g/l in 20% PBS/glycerol; Sigma).

2.3. Analyses

2.3.1. Microscopy

All retinae were viewed using a scanning Leica Confocal Microscope and TCSNT software, v. 1.6.587. The FCM was identified as a relatively S-cone free region temporal to the OD (Fig. 1). The region of retina between the OD and fovea (inclusive)—the 'Fovea-OD strip'—was imaged using a 16× objective, scanning fields 625×625 μm. Montages of the Fovea-OD strip were prepared from these images using Adobe Photoshop v.5.5. Selected areas within the same region were also scanned using a 40× objective (field size 250×250 μm).

2.3.2. Quantitative analyses

Montages were used to estimate the distance between the OD and fovea. Because this distance varies to some degree between individuals and over time we used *relative position* (expressed as a percentage) along a notional

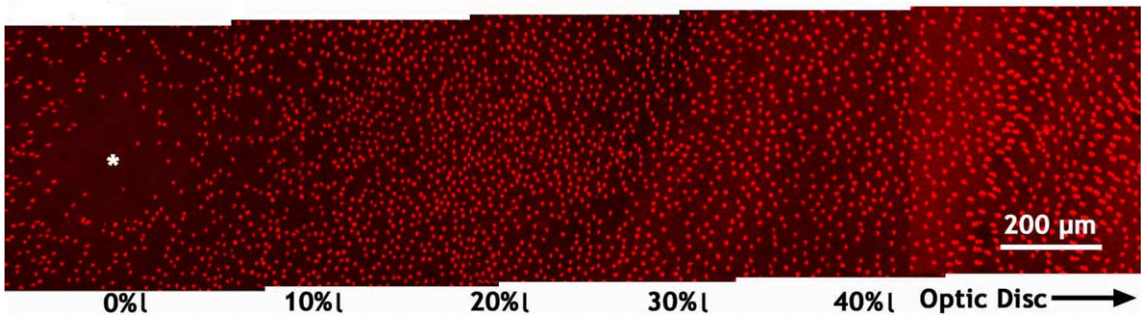

Fig. 1. Montage showing the distribution of cones immunoreactive for short-wavelength-sensitive opsin (S-cones) in a human fetal retina at 24 WG. The foveal region, which is virtually S-cone free, is to the left (asterisk), OD to the right. Percentages represent relative distance from the fovea to the OD.

line (l) connecting the FCM and OD (where the FCM is at 0% l, and the OD at 100% l) to compare S-cone density distributions. Density of S-cones and, in selected areas, average cone diameter were estimated using Scion Image (http://www.scioncorp.com).

The density recovery profile (DRP) (Rodieck, 1991) was used to assess S-cone distributions in each sample in the Fovea-OD strip using MacDRP (v.3, courtesy Bob Rodieck). Using this method an estimate of packing factor (PF), which varies between 0 (random distribution) and 1 (triangular array), is obtained that is independent of the spatial density of points in the sample. To plot PF as a function of position on the sample strip a constant binwidth of 10 μm was applied. We calculated the probability that S-cone distributions differ from random arrays in two retinal locations within the strip for each retina; a sample from the edge of the FCM ('rim'; 0.12–0.47 mm eccentricity) and a 'perifoveal' sample (1.7–3.0 mm eccentricity). In these analyses binwidth was varied to obtain a reliability factor (K) ~5.0 (Rodieck, 1991) to facilitate direct comparison of the present data with those of Martin et al. (2000).

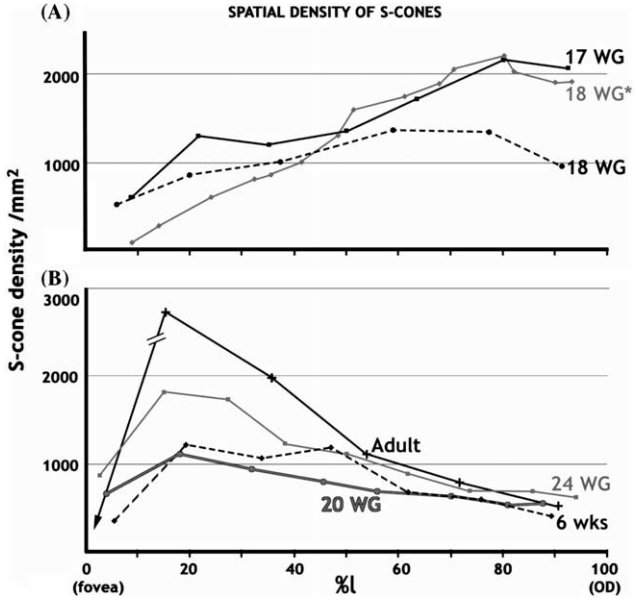

Fig. 2. A. Graphs showing the spatial density of S-cones along the fovea-OD strip in each retina studied. (A) In retinae <20 WG the peak cone density was close to the OD and density gradually declined towards the FCM. (B) In retinae ⩾20 WG peak cone density was located farther temporal, closer to the FCM. The broken arrow on the 'adult' curve indicates the projected S-cone density which, for technical reasons, could not be counted close to the fovea.

3. Results

3.1. Spatial density of S-cones

A mosaic of cones immunoreactive for S-opsin was detected throughout the Foveal-OD strip in all specimens. In general, the density distribution of S-cones was non-uniform with a clearly identifiable, S-cone poor region in the FCM, as shown in Fig. 1 in a 24 WG retina (see also Bumsted & Hendrickson, 1999). Estimates of the spatial density of S-cones across the length of the fovea-OD strips are shown in Fig. 2A and B. In two specimens of 17 and 18 WG peak spatial density of S-cones was located close to the OD (>80% l) at eccentricities of ~2.8 and ~2.0 mm, respectively. In a second retina at 18 WG peak S-cone density was located somewhat closer to the fovea at ~1.7 mm eccentricity (Fig. 2A). In all other retinae (20 WG to adult) peak spatial density of S-cones was located close to the FCM (<20% l) (Fig. 2B). Eccentricity of peak S-cone density plotted as a function of age shows a progressive 'shift' in peak spatial density of S-cones towards the fovea with increasing age (Fig. 3).

3.2. Order in the human S-cone mosaic

Mean S-cone diameters from four prefoveate retinae are shown in Fig. 4A. Examples of plots of actual S-cone distributions sampled near the FCM ('rim'—<0.5 mm eccentricity) and in the perifovea (>1.5 mm eccentricity), along with MacDRP output for those samples, are

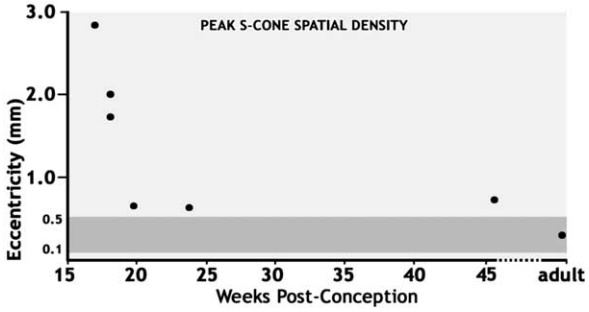

Fig. 3. A plot showing the locations of peak S-cone density in mm eccentricity from the fovea at different ages. Peak S-cone density is located at >1.7 mm eccentricity in three retinae <20 WG and <0.7 mm eccentricity in three retinae $\geqslant$ 20 WG. The highlight band shows the range of eccentricities for peak S-cone density in adult retina (Curcio et al., 1991).

shown in Fig. 4B and C, respectively. MacDRP output shows the nearest neighbour (NN) histograms (Fig. 4B and C, dark grey histogram) and the DRP (Fig. 4B and C, light tan histogram) of the sample distributions. It also shows the *effective radius* (ER, a measure of the average intercell distance) and *maximum radius* (MR, the maximum intercell distance that can be achieved with hexagonal packing at the same average spatial density) of points in the sample area (Rodieck, 1991). PF is the ratio $(ER/MR)^2$ and is a measure of deviation from a triangular array that varies between 0 (random) and 1 (triangular), independent of spatial density (Rodieck, 1991). The sample in Fig. 4B shows a skewed distribution of S-cone NN in the 'rim' sample (Fig. 4B, at ~6% l) and a low PF value of 0.15—suggesting a near-random distribution of cells. In contrast, the sample distribution from perifovea (Fig. 4C, at ~60% l) is less skewed and has a higher PF of 0.4. This apparent difference in PF between 'rim' and 'perifoveal' samples shown in Fig. 4 was common to all of the retinae studied (Table 1). In developing retinae PF ranged between 0.05 (rim at 6 weeks postnatal) and 0.4 (perifovea at 18 WG). In each retina PF was lowest in the 'rim' sample and highest between 50% and 70% of the distance along the fovea-OD strip (l), (data not shown).

The probability that S-cone distributions vary from a random array was calculated for samples obtained from

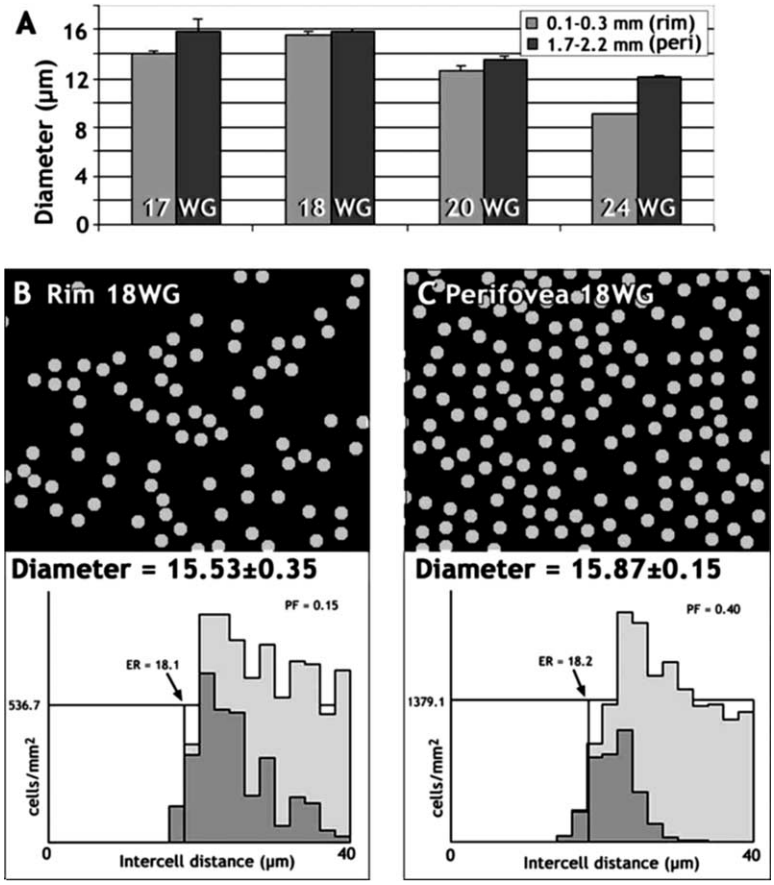

Fig. 4. A. S-cone diameters obtained from two sample areas in four of the retinae analysed in the present study. (B, C) The S-cone distributions in regions adjacent to the FCM ('rim', B) and in the perifovea (C) of an 18 WG retina, along with Mac DRP output. The density recovery profiles (DRP) are shown in light grey and the distribution of 'nearest neighbours' (NN) in the dark grey histograms. The low packing factor (PF, 0.15) obtained from sample area 'B' reflects the skewed NN distribution. The higher PF of 4.0 obtained from sample area 'C' suggests a more ordered array in the perifovea.

Table 1
Data obtained from MacDRP analysis of 6 retinae used in this study, compared with data from Martin et al. (2000). ER, effective radius; MR, maximum radius; PF, packing factor; K, reliability. *P*1 is the probability of the distribution being significantly different from a random array, without excluding S cone diameter as a variable. *P*2 is a recalculation of this probability, after subtracting S cone diameter from the ER value. Only samples from the perifovea in retinae 20 WG or older are significantly different from a random array

Age	Eccentricity (mm)	Points	Density (mm^2)	ER	MR	PF	K	ER/Δ*R*	*P*1	S-cone diameter (μm)	ER-diameter	ER-diameter/Δ*R*	*P*2
17 WG	0.30 rim	155	652.6	14.8	42.1	0.12	5.1	1.64	<0.01	14.06	0.74	0.08	>0.2
	1.77 perifovea	353	1367.9	16.8	29.1	0.33	4.9	4.20	<0.01	15.96	0.84	0.21	>0.2
18 WG	0.17 rim	204	536.7	17.5	46.4	0.14	5.3	1.94	<0.01	15.53	1.97	0.22	>0.2
	1.67 perifovea	525	1379.1	17.9	28.9	0.38	4.5	5.97	<0.01	15.87	2.03	0.68	>0.2
20 WG	0.16 rim	255	668.8	17.5	41.6	0.18	5.1	2.50	<0.01	12.61	4.89	0.70	>0.1
	2.03 perifovea	266	697.6	21.7	40.7	0.28	5.3	3.10	<0.01	13.58	8.12	1.16	<0.05*
24 WG	0.12 rim	339	886.2	14	36.1	0.15	4.9	2.80	<0.01	9.02	4.98	1.00	>0.05
	2.27 perifovea	435	1131.6	16.9	31.9	0.28	5	4.23	<0.01	12.12	4.78	1.20	<0.05*
6 Weeks	0.23 rim	135	361	13	56.6	0.05	5.1	1.00	<0.1	7.00	6.00	0.46	>0.2
	2.52 perifovea	258	676.6	22	41.3	0.28	5.2	3.14	<0.01	7.00	15.00	2.14	<0.01*
Adult 1	0.47 rim	1057	2740.9	8.9	20.5	0.19	6	4.45	<0.01	7.00	1.90	0.95	>0.05
	1.62 perifovea	428	1109.8	12.3	32.3	0.15	4.9	3.08	<0.01	7.00	5.30	1.33	<0.05*
Adult 2[a]	0.40 rim	167	2224	9.5	22.8	0.18	5.4	1.90	<0.01	7.00	2.50	0.50	>0.2
	3.00 perifovea	184	711	20.8	40.3	0.27	5.1	2.60	<0.01	7.00	13.80	1.73	<0.01*

* Denotes significance at the 5% level.
[a] Data from Martin et al. (2000).

'rim' and 'perifovea' locations in each retina (see Rodieck, 1991, Table 1). The results show that when cone cell body size is not taken into account, the S-cone array is significantly different from a random distribution at both locations ('rim' and 'perifovea') at all ages (Table 1: $P1 < 0.01\%$).

It has been suggested, however, that cell diameter is an important variable in NN and DRP estimates (Martin et al., 2000). We therefore used mean S-cone diameters measured directly from immunoreactive cell bodies in each sample area in fetal retinae (Table 1, S-cone diameter) and subtracted these from the ER. In older specimens S-opsin is present only in the cone outer segments and an estimate of S-cone diameter (7.0 μm) was used (see also Martin et al., 2000). In retinae younger than 20 WG, when cone size is taken into account, the probability of S-cone distributions varying from a random array is not significant at either sample location (Table 1, *P*2). A similar result was found for S-cone samples taken from the 'rim' of retinae 20 WG or older. However, samples from the perifovea of retinae 20 WG or older were found to be significantly different from a random array when soma diameter was taken into account (Table 1, $P2 < 0.05\%$).

4. Discussion

In this study we investigate changes in S-cone density and spatial arrangement during development in a sample area of central retina. The selected region is easy to compare between retinae of different ages, being defined by two major landmarks—the fovea and OD. Furthermore, a relatively small amount of retinal growth is attributed to this region as the eye increases in size, with proportionally more retinal area being added in peripheral regions (Packer et al., 1990; Provis & van Driel, 1985; Steineke & Kirby, 1993). The results are discussed in relation to (1) development of the cone topography, and (2) randomness vs order in the human S-cone array.

4.1. Development of cone topography

In human retina cones are identifiable first at the incipient fovea at around 11 WG (Linberg & Fisher, 1990) and at this age a subset of cones on the edge of the FCM expresses the short-wavelength-sensitive opsin (Xiao & Hendrickson, 2000). This contrasts with the majority of L/M cones in the FCM that express opsin several weeks later (Xiao & Hendrickson, 2000). Some S-cones can be detected near the OD as early as 13WG (Xiao & Hendrickson, 2000) but the spatial density of immunoreactive S-cones at this location rises between 13 and 16 WG, suggesting that S-cones are added and/or S-opsin is expressed at this location over a period of approximately 3 weeks (Cornish et al., in press; Xiao & Hendrickson, 2000). However, very few S-cones are added to the cone mosaic in the vicinity of the OD after

17 WG (Cornish et al., in press). For this reason retinae younger than 17 WG were not included in the study.

Recently we found that near the OD S-cone density declines rapidly from approximately 2000 mm^{-2} at 16 WG to 1000 mm^{-2} at 18 WG, followed by a slower decline to around 500 S-cones/mm^2 by birth. Our data showed that this decline is not due to natural cell death. This finding is in agreement with a previous study where very low levels of apoptosis were evident in the ONL of retinal sections (Georges, Madigan, & Provis, 1999). Based on the results of both studies (Cornish et al., in press; Georges et al., 1999) we cautiously estimate the levels of apoptosis in the cone population during this period to be <0.01%.

In the present study we observe that the decline in S-cone density near the OD between 17 and 20 WG is accompanied by *increases* in S-cone density at locations closer to the FCM (Fig. 2A and B). Indeed, the analysis of the eccentricity of peak S-cone density in each retina demonstrates a centripetal 'shift' during development, from locations close to the OD in retinae <20 WG to eccentricities close to the adult range (Curcio et al., 1991) by 20 WG (Fig. 3). We conclude that this change in the S-cone spatial density distribution is attributable to early displacements of the photoreceptor population towards the incipient fovea (centripetal displacement), and that this displacement accounts for the drop in S-cone density near the OD (Cornish et al., in press).

A high density of cones in the FCM is fundamental to achieving high visual acuity and several studies have suggested that the region of high cone density at the fovea results from centripetal displacement of photoreceptors. Hendrickson and Kupfer (1976) used sections through the FCM of fetal macaque retina, measuring the distance from the center of FCM to the nearest group of rod nuclei on both nasal and temporal sides to show that between fetal day (Fd) 74 and approximately 50 days postnatal, the diameter of the 'rod free' area ('FCM', this study) was reduced from 1600 μm to approximately 300 μm. A similar study of human retinae found that the 'rod free' area reduced in size from 1600 μm (diameter) at 22 WG, to an adult value of 650–700 μm by 45 months postnatal, associated with a rise in the peak spatial cone density from 18,500 mm^{-2} at 22 WG to 36,000 mm^{-2} at 1 week postnatal (*P*1 week) (Yuodelis & Hendrickson, 1986). A study using retinal wholemounts showed a gradient of cone densities and diameters across the FCM from an early age, and a rise in peak spatial cone density from approximately 14,000 mm^{-2} at 13 WG, to approximately 38,000 mm^{-2} at 24 WG in the human (Diaz-Araya & Provis, 1992). It is also established that these increases occur in the absence of cell division (LaVail, Rapaport, & Rakic, 1991; Provis et al., 1985; Sandercoe et al., 1999).

Through analysing cones within the FCM these studies show that from around 13 WG in the human, cones accumulate at a focal point within the FCM (Diaz-Araya & Provis, 1992; Hendrickson, 1994; Hendrickson & Kupfer, 1976; Yuodelis & Hendrickson, 1986). A further order of magnitude increase in cone density is achieved in the postnatal period after the foveal depression has formed (Hendrickson, 1994; Hendrickson & Kupfer, 1976; Packer et al., 1990; Yuodelis & Hendrickson, 1986). Using changes in the S-cone population as an indicator of photoreceptor displacement, the present results suggest that centripetal displacement of photoreceptors affects a large area of retina, extending at least as far as the eccentricity of the OD (3–3.5 mm).

The present findings, however, provide no data which help us to gain insight into what the mechanisms underlying cone displacement may be. It has been suggested that mechanical factors, resulting from greater relative stretch in the avascular foveal region, may underpin increases in foveal cone density during formation of the foveal depression (Springer, 1999; Springer & Hendrickson, 2004). However, previous data show that cone density within the FCM increases significantly prior to definition of the foveal avasular zone, at around 25 WG in humans, while the present data indicate that displacement of cones from the region near the OD towards the FCM is occurring prior to 20 WG. Our hypothesis is that morphological specialization of cones, mediated by molecular mechanisms that result in narrowing and elongation, enhance cone packing and are responsible for the changes in cone density distributions shown here (Fig. 2). Further studies are in progress in this area. Eye growth and retinal stretching may also contribute to cone packing (Springer & Hendrickson, 2004).

4.2. Order in the S-cone array

Several studies have investigated order in primate S-cone arrays (Ahnelt et al., 1987; Curcio et al., 1991; Marc & Sperling, 1977; Martin & Grunert, 1999; Martin et al., 2000; Roorda & Williams, 1999; Roorda et al., 2001; Shapiro, Schein, & de Monasterio, 1985). An analysis of Voronoi neighbours in the S-cone population of adult human retina indicates that S-cones at an eccentricity of 0.35 mm are irregularly distributed, while at an eccentricity of 3 mm the S-cone distribution is 'moderately regular' (Curcio et al., 1991). Martin et al. (2000) drew similar conclusions using the DRP analysis of the same sample areas used by Curcio et al. (1991), and Roorda and colleagues also find that S-cones near the fovea are distributed in a pattern that is indistinguishable from random (Roorda et al., 2001). Sample locations used in each of those studies are consistent with our definitions for 'rim' and 'perifoveal' samples,

respectively. Using the DRP analysis of adult retina, we also find 'rim' samples to resemble a random distribution and 'perifoveal' samples to be significantly different from a random distribution consistent with previous findings (Table 1).

Our analyses of developing retinae indicated that in all specimens PF was lowest in samples adjacent to the FCM. We also found low to intermediate PF values in each retina in samples close to the OD, but mechanical distortion of these sample regions caused by proximity to the OD may have some impact on spatial order (not shown). Overall, plots of PF against distance in the Foveal-OD strip are bow-shaped, with the higher values tending to occur in the middle of the strip, in the perifovea. Our statistical analyses confirm that the S-cone distribution on the edge of the FCM is random throughout development and that this is maintained into adulthood. However, in the perifovea, S-cone distributions that initially are random (17 and 18 WG), are non-random by 20 WG (Table 1, *P*2).

It was suggested previously that irregularity in the S-cone mosaic near the fovea may be due to disruption of regular S-cone spacing by "cone migration" (Roorda & Williams, 1999), implying that S-cone distributions are inherently regular, but become disordered around the FCM as a result of cone displacements. Contrary to this, the present analysis of fetal S-cones suggests that the S-cone distribution is *inherently* random (17 and 18 WG, Table 1, *P*2) and instead becomes more ordered in the perifovea with age. Our data indicate that by 20 WG the S-cone distribution is 'adult-like', being random around the FCM but ordered in the perifovea, and having a peak density close to the FCM, as in adult retina (Curcio et al., 1991; Martin et al., 2000; present study). S-cone density data also demonstrate a significant change in the S-cone density distribution after 18 WG, in that it too is 'adult-like' by 20 WG (Fig. 2B).

These findings suggest that the spatial distribution of S-cones (density and order) undergo major changes early in development. These changes include a reversal of the spatial density gradient between the FCM and OD and the establishment of order in regions $>\sim$2.0 mm from the FCM. These changes in the S-cone population likely reflect similar changes in the entire photoreceptor population of this region. Significantly, these patterns are established by 20 WG, some 5 weeks before the foveal depression begins to form. On this basis, these early changes in spatial density and order appear to be part of a process associated with specialization of the photoreceptor mosaic and FCM, and not with development of the foveal depression per se. We suggest, therefore, that early in development there is an underlying molecular mechanism associated with adaptation of the photoreceptor layer that is independent of 'mechanical' events that may impact on or promote formation of the foveal depression at a later stage.

Acknowledgements

The authors thank Bob Rodieck for the MacDRP software, Jeremy Nathans for the antibody against S opsin, and Paul Martin for advice and useful comments on an early draft of the manuscript. Richard Stump gave valuable statistical advice. Thanks also to Bernie Tuch and his staff, and Eye Bank co-ordinators for making the study possible.

References

Ahnelt, P. K., Kolb, H., & Pflug, R. (1987). Identification of a subtype of cone photoreceptor, likely to be blue sensitive, in the human retina. *Journal of Comparative Neurology, 255*, 18–34.

Bumsted, K., & Hendrickson, A. (1999). Distribution and development of short-wavelength cones differ between Macaca monkey and human fovea. *Journal of Comparative Neurology, 403*, 502–516.

Chiu, M. I., Zack, D. J., Wang, Y., & Nathans, J. (1994). Murine and bovine blue cone pigment genes: Cloning and characterization of two new members of the S family of visual pigments. *Genomics, 21*, 440–443.

Cornish, E. E., Xiao, M., Yang, Z., Provis, J. M., & Hendrickson, A. (in press). Opsin co-expression and the role of apoptosis in determining cone types in the developing human retina. *Experimental Eye Research*.

Curcio, C. A., Allen, K. A., Sloan, K. R., Lerea, C. L., Hurley, J. B., Klock, I. B., & Milam, A. H. (1991). Distribution and morphology of human cone photoreceptors stained with anti-blue opsin. *Journal of Comparative Neurology, 312*, 610–624.

Diaz-Araya, C. M., & Provis, J. M. (1992). Evidence of photoreceptor migration during early foveal development: A quantitative analysis of human fetal retinae. *Visual Neuroscience, 8*, 505–514.

Georges, P., Madigan, M. C., & Provis, J. M. (1999). Apoptosis during development of the human retina: Relationship to foveal development and retinal synaptogenesis. *Journal of Comparative Neurology, 413*, 198–208.

Hendrickson, A. (1994). Primate foveal development: A microcosm of current questions in neurobiology. *Investigative Ophthalmology and Visual Science, 35*, 3129–3133.

Hendrickson, A., & Kupfer, C. (1976). The histogenesis of the fovea in the macaque monkey. *Investigative Ophthalmology, 15*, 746–756.

LaVail, M. M., Rapaport, D. H., & Rakic, P. (1991). Cytogeneis in the monkey retina. *Journal of Comparative Neurology, 309*, 86–114.

Linberg, K. A., & Fisher, S. K. (1990). A burst of differentiation in the outer posterior retina of the eleven-week human fetus: An ultrastructural study. *Visual Neuroscience, 5*, 43–60.

Marc, R. E., & Sperling, H. G. (1977). Chromatic organization of primate cones. *Science, 196*, 454–456.

Martin, P. R., & Grunert, U. (1999). Analysis of the short wavelength-sensitive ("blue") cone mosaic in the primate retina: Comparison of New World and Old World monkeys. *Journal of Comparative Neurology, 406*, 1–14.

Martin, P. R., Grunert, U., Chan, T. L., & Bumsted, K. (2000). Spatial order in short-wavelength-sensitive cone photoreceptors: A comparative study of the primate retina. *Journal of the Optical Society of America, A, Optics, Image Science, and Vision, 17*, 557–567.

Packer, O., Hendrickson, A. E., & Curcio, C. A. (1990). Developmental redistribution of photoreceptors across the *Macaca nemestrina* (pigtail macaque) retina. *Journal of Comparative Neurology, 298*, 472–493.

Provis, J. M., & van Driel, D. (1985). Retinal development in humans: The roles of differential growth rates, cell migration and naturally

occurring cell death. *Australian and New Zealand Journal of Ophthalmology, 13*, 125–133.

Provis, J. M., van Driel, D., Billson, F. A. B., & Russell, P. (1985). Development of the human retina: Patterns of cell distribution and redistribution in the ganglion cell layer. *Journal of Comparative Neurology, 233*, 429–451.

Robinson, & Hendrickson (1995). Shifting relationships between photoreceptors and pigment epithelial cells in monkey retina: Implications for the development of retinal topography. *Visual Neuroscience, 12*, 767–778.

Rodieck, R. W. (1991). The density recovery profile: A method for the analysis of points in the plane applicable to retinal studies. *Visual Neuroscience, 6*, 95–111.

Roorda, A., Metha, A. B., Lennie, P., & Williams, D. R. (2001). Packing arrangement of the three cone classes in primate retina. *Vision Research, 41*, 1291–1306.

Roorda, A., & Williams, D. R. (1999). The arrangement of the three cone classes in the living human eye. *Nature, 397*, 520–522.

Sandercoe, T. M., Madigan, M. C., Billson, F. A., Penfold, P. L., & Provis, J. M. (1999). Astrocyte proliferation during development of the human retinal vasculature. *Experimental Eye Research, 69*, 511–523.

Shapiro, M. B., Schein, S. J., & de Monasterio, F. M. (1985). Regularity and structure of the spatial pattern of blue cones of macaque retina. *Journal of the American Statistical Association, 80*, 803–812.

Springer, A. D. (1999). New role for the primate fovea: A retinal excavation determines photoreceptor deployment and shape. *Visual Neuroscience, 16*, 629–636.

Springer, A. D., & Hendrickson, A. (2004). Development of the primate fovea. 1. Modeling the role of mechanical variables in pit formation. In press.

Steineke, T. C., & Kirby, M. A. (1993). Early axon outgrowth of retinal ganglion cells in the fetal rhesus macaque. *Brain Research, Developmental Brain Research, 74*, 151–162.

Wang, Y., Macke, J. P., Merbs, S. L., Zack, D. J., Klaunberg, B., Bennett, J., Gearhart, J., & Nathans, J. (1992). A locus control region adjacent to the human red and green visual pigment genes. *Neuron, 9*, 429–440.

Williams, D. R., MacLeod, D. I. A., & Hayhoe, M. H. (1981). Foveal tritanopia. *Vision Research, 21*, 1341–1356.

Xiao, M., & Hendrickson, A. (2000). Spatial and temporal expression of short, long/medium, or both opsins in human fetal cones. *Journal of Comparative Neurology, 425*, 545–559.

Yuodelis, C., & Hendrickson, A. (1986). A qualitative and quantitative analysis of the human fovea during development. *Vision Research, 26*, 847–855.